3D Passive Marker Tracking for MR-Guided Interventions

F. Maier[1], A. J. Krafft[1], R. J. Stafford[2], J. P. Yung[2,3], R. Dillmann[4], W. Semmler[1], and M. Bock[1]
[1]Medical Physics in Radiology, German Cancer Research Center (DKFZ), Heidelberg, Germany, [2]Department of Imaging Physics, The University of Texas M. D. Anderson Cancer Center, Houston, Texas, United States, [3]The University of Texas Graduate School of Biomedical Sciences, Houston, Texas, United States, [4]Institute of Anthropomatics, Karlsruhe Institute of Technology, Karlsruhe, Germany

Introduction

In MR-guided interventions, fast and robust localization of the instruments is mandatory. Active tracking techniques with small radio-frequency coils are not applied in clinical practice due to safety hazards from RF-induced heating [1]. In contrast to active tracking, a passive tracking technique with a cylindrical marker has been proposed for fast and safe localization of linear instruments, such as biopsy needles [2]. This technique employs a phase-only cross correlation (POCC) algorithm to detect the position of the passive marker from two tracking images aligned orthogonally to the direction of the device.

One limitation of this tracking approach occurs if the marker is moved in the direction of its symmetry axis (needle direction, Fig. 1) as this degree of freedom is not tracked by POCC. To overcome this restriction, two extended pulse sequences have been proposed recently [3, 4] using modified markers. In this work, an accelerated passive marker tracking sequence is introduced, which detects the 3D position of the marker without the need of any hardware modifications.

Materials and Methods

All experiments were carried out on a clinical 1.5 T whole body MR system (Magnetom Avanto, Siemens, Erlangen, Germany) using standard imaging RF coils. The passive cylindrical marker (Invivo GmbH, Schwerin, Germany) was originally designed for prostate biopsies. The marker (diameter: 12 mm, length: 80 mm) features a central opening (3 mm) for the insertion of a puncture needle, and is filled with contrast agent solution (Gd-DTPA/H_2O 1:100).

Pulse Sequence: Based on the POCC tracking pulse sequence [2], an improved and more flexible tracking sequence was implemented. Two parallel tracking slices orientated perpendicular to the marker direction (cf. Fig. 1, 2) were acquired (FLASH, parameters: TR/TE = 3.2/1.5 ms, α = 15°, FOV: 300×300 mm, matrix: 192×144, partial Fourier: 5/8) with a slice thickness of up to 20 mm to improve the SNR for the tracking algorithm. Each slice showed the marker as a ring structure, which was detected subsequently in each tracking image based on the POCC algorithm [5]. The mask generation has been improved to operate with anisotropic sized pixels allowing for a reduction of the resolution in phase-encoding direction and thus for an increase in acquisition speed. Pixels at the edges of the mask images were interpolated using *1 + cosine* to enhance the magnitude maxima in POCC results. Additionally, robustness was improved by testing the positive sign of the real part of the POCC-result at the positions where the POCC-magnitude shows a local maximum. Finally, sub-pixel accuracy was achieved by center-of-mass calculations [2]. The position of the imaging plane (Fig. 3) was aligned with the marker and was displayed every 0.9 s.

3D Position Detection Algorithm: According to the detected marker positions within the tracking slices (p_1, p_2, Fig. 1) the image plane (trueFISP, TR/TE = 3.2/1.5 ms, α = 75°, FOV: 300×300 mm, matrix: 192×144, partial Fourier: 5/8) was automatically aligned parallel to the marker direction. Additionally, the needle axis was calculated and projected into the imaging plane (cf. Fig. 1). Next, a region of interest (ROI) was defined around the assumed position of the marker within the imaging plane (ROI size: marker diameter × 2 · marker length) with the ROI center located at (p_1 + p_2) / 2. The magnitude values of all pixels within the ROI were projected to the estimated needle axis, to determine the position of the marker in direction of the needle. Afterwards, a threshold approach was applied to detect the edges of the marker within the projection data (magnitude threshold: 20% of mean signal between p_1 and p_2).

Edge detection was started at the ROI center (p_1 + p_2) / 2 and was applied in both directions. After detection of both edges a plausibility check was applied to reject invalid positions: The detected length must not deviate more than 20 % from the actual marker length. In case of detection failure the center of the marker is assumed at the ROI center. Finally, the 3D center position of the marker and its orientation were sent from the image reconstruction system to the scanner, and the position and orientation of the tracking slices were updated prior to the next tracking cycle.

Experiment: The precision of the 3D localization technique was evaluated by performing 100 tracking steps at a fixed position. The standard deviation of the needle target position in a typical penetration depth of 80 mm was evaluated. Additionally, the robustness of the 3D position detection during motion was tested. The marker was moved 30 cm in the needle direction and 45° from the needle direction inside the scanner.

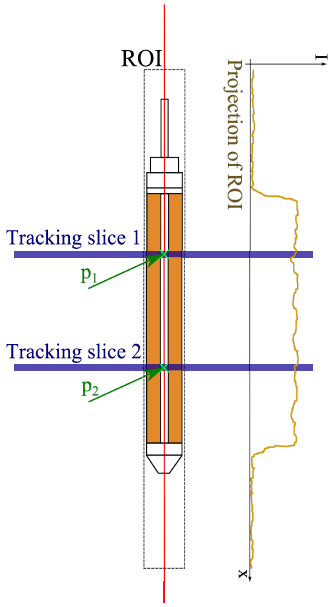

Fig. 1: *Cylindrical marker filled with contrast agent solution (orange), needle axis (red), tracking slices (blue), marker positions in tracking slices (green), and projection of region of interest (ROI) for position detection in needle direction.*

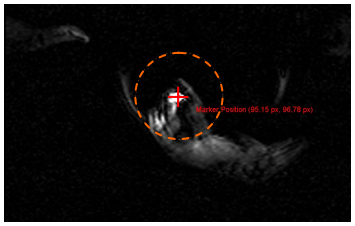

Fig. 2: *Tracking slice (cf. Fig 1) containing ring structure, marker position (red cross) and search ROI (orange).*

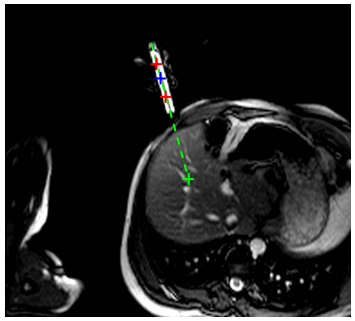

Fig. 3: *Imaging slice showing marker and theoretical needle trajectory overlay (green) (FOV: 400×400 mm).*

Results and Discussion

At the fixed marker position, deviations of the needle target position of 0.3 mm perpendicular to the needle axis and 1.1 mm parallel to the needle axis were measured. The maximum velocity, at which the marker was able to be continuously tracked, was 2.2 cm/s and 1.9 cm/s for motion in the needle direction and 45 degrees offset from the needle direction, respectively.

The total acquisition time for two tracking slices and one imaging slice was reduced to 0.9 s. Position detection in the needle direction enhanced the robustness of the tracking sequence, since the position of the tracking slices was updated if there was through-plane motion. Additionally, the target position of the needle tip was visualized. In the case of strong trueFISP banding artifacts perpendicular to the marker direction, the proposed algorithm could fail. However, the plausibility check avoided using this corrupted data for position updates, since the detected length was shorter than expected.

In conclusion, the proposed technique allows for an accelerated and robust 3D passive marker tracking without hardware modifications (as described in [3, 4]). Thus, the choice of an optimal needle trajectory in percutaneous interventions is highly facilitated and under manual control of the operator.

References

[1] Konings MK, *et al.* J Magn Reson Imaging. 2000; 12: 79-85.
[2] de Oliveira *et al.* Magn Reson Med. 2008; 59: 1043-1050.
[3] de Oliveira *et al.* In: Proc 16th Annual Meeting ISMRM, Toronto, 2008.
[4] Maier *et al.* In: Proc 17th Annual Meeting ISMRM, Honolulu, 2009.
[5] Chen Q, *et al.* IEEE Trans Pattern Anal Mach Intell 16(12):1156-1162, 1994.